

Time-delayed predator–prey and competition wavefronts. Theory and comparison to experimental observations

V. Ortega-Cejas^{a,*}, J. Fort^b, V. Mndez^c

^a*Departament de Física, Universitat Autònoma de Barcelona, 08193 Bellaterra, Barcelona, Spain*

^b*Departament de Física, Universitat de Girona, 17071 Girona, Spain*

^c*Departament de Medicina, Universitat Internacional de Catalunya, 08190 Sant Cugat del Vallès, Barcelona, Spain*

Received 25 May 2005

Available online 17 November 2005

Abstract

The effect of the delay time on the speed of wave fronts for interacting–diffusing models is studied analytically and numerically, both for predator–prey and competition models. It is shown that the interaction parameters may be evaluated from the time during which both species coexist until one of them is driven to extinction. We also compare our predicted speeds with experimental measurements for two biophysical systems. In both cases we find good agreement.

© 2005 Elsevier B.V. All rights reserved.

Keywords: Time-delayed reaction-diffusion; Biological invasions; Wavefronts speed

1. Introduction

Interactions between two species which interact, react (or reproduce) and diffuse have been a widely treated topic in the Physics and Biology literature [1]. Wavefronts are special solutions characterized by a constant shape and asymptotic speed and they connect two steady states. In this paper we will focus on the problem of their speed. The main novelty is introducing a delay time to diffusive fluxes that will lead in practice to the replacement of the classical Fick's diffusion law by a Maxwell–Cattaneo equation. In contrast to Fick's law, causality is preserved [2]. As a result of this change, differential equations for number densities of particles or individuals will be hyperbolic instead of parabolic. Hyperbolic reaction–diffusion equations (HRDEs) have the main conceptual advantage of predicting finite speeds for all kind of physical signals, contrary to what parabolic reaction–diffusion equations (PRDE) do [2]. Al-Ghoul and Eu have analyzed the Turing instability [3] and the pattern formation [4] of HRDE for cubic reversible reactions. On the other hand, both microscopic derivations and experimental data [5–7] consistently show that, due to the finite intergeneration interval of biological populations, diffusion cannot be accurately described classically, but time-delayed equations must be used instead. In contrast to previous studies on diffusing Lotka–Volterra systems [1,8–13], we will take this time-delayed effect into account by deriving the corresponding evolution equations. Our new model is introduced in Section 2. We determine the wavefront speed analytically in Section 3, where we also check it by

*Corresponding author. Fax: +34935812155.

E-mail address: vicente.ortega@uab.es (V. Ortega-Cejas).

means of numerical integrations of the evolution equations. In Section 4 we apply our results to two different biophysical systems, and find good agreement to experimental data in both cases. In contrast to all previous studies, the interaction parameter among the species is evaluated from experimental data different from the wavefront speed (specifically, we will determine it from the species coexistence time). This allows us to find good agreement to observations *without using any free or adjustable parameters*. As far as we know, this is done here for the first time. This is clearly a very relevant problem, in the sense that its solution is necessary to compare predicted front speeds to experiment. Thus, it is rather surprising that it was previously unsolved not only of time-delayed, but also for the classical (i.e., non-delayed or Fickian) approach. Section 5 is devoted to concluding remarks.

2. Time-delayed diffusive interacting species

Let $N(x, t)$ and $M(x, t)$ stand for number densities of two interacting species that diffuse, interact and react (or reproduce), x being the Cartesian position coordinate and t the time. For the moment, let us consider one-dimensional systems (the two-dimensional case will be tackled in Section 4). In order to drive the space–time dynamics, we assume the general balance equations for number densities and the Maxwell–Cattaneo type for the diffusive fluxes,

$$\frac{\partial N}{\partial t} + \frac{\partial J^{(N)}}{\partial x} = F(N) \pm \Gamma NM, \quad (1)$$

$$\tau \frac{\partial J^{(N)}}{\partial t} + J^{(N)} = -D \frac{\partial N}{\partial x}, \quad (2)$$

$$\frac{\partial M}{\partial t} + \frac{\partial J^{(M)}}{\partial x} = \hat{F}(M) - \hat{\Gamma} NM, \quad (3)$$

$$\hat{\tau} \frac{\partial J^{(M)}}{\partial t} + J^{(M)} = -\hat{D} \frac{\partial M}{\partial x}, \quad (4)$$

where $F(N)$ and $\hat{F}(M)$ are source functions (they mean the net number of individuals that appear per unit time and length for the corresponding species), $J^{(N)}$ and $J^{(M)}$ are diffusion fluxes, D and \hat{D} are diffusion coefficients and τ and $\hat{\tau}$ are relaxation (or delay) times. The last term in (1) and (3) takes care of the interactions between both species. We have assumed, as usual [1,8–13], a weak interaction between them, which corresponds to keeping only the lowest non-vanishing order in the interaction function, when developed in a Taylor series with two independent variables (N and M). The positive sign in Eq. (1) refers to prey–predator interaction [14]. In this first case, the interaction involves an increase in the density $N(x, t)$ and a decrease in $M(x, t)$. This is the reason to call N predator density and M prey density. The second case corresponds to the minus sign in Eq. (1), and is referred to as competition because the interaction leads to a decrease of both N and M . A specific application of the predator–prey case and of the competition one will be presented in Section 4. On the other hand, Eqs. (2) and (4) have been derived in a variety of ways [5]. For biophysical application purposes, it is very important to stress that (as shown in Ref. [6]) the value of τ (and, analogously, $\hat{\tau}$) equals half the mean time interval between two subsequent generations (of the corresponding species). Combining Eqs. (1)–(4), it is not difficult to arrive at equations in which the diffusive fluxes no longer appear,

$$\tau N_{tt} + \{1 - \tau[F'(N) \pm \Gamma M]\} N_t = DN_{xx} + F(N) \pm \Gamma(M + \tau M_t)N, \quad (5)$$

$$\hat{\tau} M_{tt} + \{1 - \hat{\tau}[\hat{F}'(M) - \hat{\Gamma} N]\} M_t = \hat{D}M_{xx} + \hat{F}(M) - \hat{\Gamma}(N + \hat{\tau} N_t)M, \quad (6)$$

with $F'(N) = \partial F/\partial N$ and $\hat{F}'(M) = \partial \hat{F}/\partial M$. A more elaborated derivation of HRDE can be found in Ref. [3]. In the classical approach, namely $\tau = \hat{\tau} = 0$, the usual diffusive Lotka–Volterra (or PRDE) equations for prey–predator and competition models are recovered. However, for several single-species biophysical systems it has been shown that such an approach is not valid since the neglected terms are quantitatively important [6,15]. Here, we will tackle the time-delayed extension to several-species systems, undergoing either predator–prey or competition dynamics.

As usual [5], in order to derive simple equations, let us assume that source functions may be written as $F(N) = kN_{max}f(n)$ and $\hat{F}(M) = \hat{k}M_{max}\hat{f}(m)$, where $1/k$ and $1/\hat{k}$ are characteristic times of the two species reproduction processes (e.g., $k = F'(0)$ for the logistic case, namely $F(N) = F'(0)N(1 - N/N_{max})$ [6]), whereas N_{max} and M_{max} are carrying capacities (i.e., the maximum possible values of the corresponding population densities for a given environment [5]). We have also defined $n = N/N_{max}$ and $m = M/M_{max}$. Introducing dimensionless coordinates $t^* = kt$ and $x^* = x\sqrt{k/D}$, Eqs. (5) and (6) become

$$an_{tt} + \{1 - a[f'(n) \pm \gamma m]\}n_t = n_{xx} + f(n) \pm \gamma(m + am_t)n, \tag{7}$$

$$\hat{a}m_{tt} + \{1 - \hat{a}[\kappa\hat{f}'(m) - \hat{\gamma}n]\}m_t = \delta m_{xx} + \kappa\hat{f}(m) - \hat{\gamma}(n + \hat{a}n_t)m, \tag{8}$$

where asterisks have been omitted for notational simplicity, and the following dimensionless parameters have been defined:

$$a = k\tau, \quad \hat{a} = k\hat{\tau}, \quad \gamma = \Gamma M_{max}/k, \quad \hat{\gamma} = \hat{\Gamma} N_{max}/k, \quad \delta = \hat{D}/D, \quad \kappa = \hat{k}/k. \tag{9}$$

Usually, $f(n)$ and $\hat{f}(m)$ are nonlinear functions with two roots, typically 0 and 1. Note that logistic growth [6] for both species, i.e., $F(N) = kN(1 - N/N_{max})$ and $\hat{F}(M) = \hat{k}M(1 - M/M_{max})$, is included in this assumption and in this case we get the well-known dimensionless growth functions $f(n) = n(1 - n)$ and $\hat{f}(m) = m(1 - m)$ [5,16].

3. Stability conditions and front speeds

The fixed points for the system (7) and (8) can be found by solving the reaction terms equal to zero, i.e.,

$$f(n) \pm \gamma nm = 0, \\ \kappa\hat{f}(m) - \hat{\gamma}nm = 0.$$

Assuming logistic growth for both species, it is easy to show that there are four fixed points given by

$$A = (n = 0, m = 0),$$

$$B = (n = 0, m = 1),$$

$$C = (m = 0, n = 1),$$

$$D = \left(n = \frac{\kappa(1 \pm \gamma)}{\kappa \pm \gamma\hat{\gamma}}, m = \frac{\kappa - \hat{\gamma}}{\kappa \pm \gamma\hat{\gamma}} \right). \tag{10}$$

State *A* means the extinction of both species, *B* and *C* correspond to extinction of one of them and *D* is a state of coexistence.

We focus on the possibility of a phase-space trajectory from steady state *B* to steady state *C*, provided that the parameters have suitable values. In non-homogeneous systems, travelling wave solutions may exist connecting both states [17]. These solutions are characterized by a constant shape and speed. We shall now derive the conditions for wavefronts to exist. As usual [5], we define variable $z = x - ct$, where $c > 0$ is dimensionless speed of the front. From Eqs. (7) to (8), we find that wavefronts with profiles $n(z) = n(x - ct)$ and $m(z) = m(x - ct)$ must satisfy the equations

$$(1 - ac^2)n_{zz} + c\{1 - a[f'(n) \pm \gamma m]\}n_z \mp c\gamma anm_z + f(n) \pm \gamma mn = 0, \tag{11}$$

$$(\delta - \hat{a}c^2)m_{zz} + c\{1 - \hat{a}[\kappa\hat{f}'(m) - \hat{\gamma}n]\}m_z + c\hat{\gamma}\hat{a}mn_z + \kappa\hat{f}(m) - \hat{\gamma}nm = 0 \tag{12}$$

and they have to obey the following boundary conditions:

$$n(z \rightarrow \infty) = m(z \rightarrow -\infty) = 0 \quad \text{and} \quad n(z \rightarrow -\infty) = m(z \rightarrow \infty) = 1. \tag{13}$$

3.1. Linear phase-space analysis

We shall follow the usual approach [1] to study the stability of the steady states, which in our case are given by Eq. (10).

On one hand, linearization of Eqs. (11) and (12) around fixed point B leads to the following expressions for the eigenvalues:

$$\lambda_{\pm}^B = \frac{-c[1 - a(1 \pm \gamma)] \pm \sqrt{c^2[1 + a(1 \pm \gamma)]^2 - 4(1 \pm \gamma)}}{2(1 - ac^2)},$$

$$\hat{\lambda}_{\pm}^B = \frac{-c(1 + \hat{a}\kappa) \pm \sqrt{c^2(1 - \hat{a}\kappa)^2 + 4\delta\kappa}}{2(\delta - \hat{a}c^2)}. \quad (14)$$

Thus, the condition for the eigenvalues to be real (to keep the number densities in the positive quadrant) is

$$c \geq \frac{2\sqrt{1 \pm \gamma}}{1 + a(1 \pm \gamma)}. \quad (15)$$

We note that for competition model, condition (15) must be satisfied only if $\gamma < 1$, otherwise no restriction can be found.

On the other hand, if linearization of Eqs. (11) and (12) around the fixed point C is made, the eigenvalues are given by

$$\lambda_{\pm}^C = \frac{-c(1 + a) \pm \sqrt{c^2(1 - a)^2 + 4}}{2(1 - ac^2)},$$

$$\hat{\lambda}_{\pm}^C = \frac{-c[1 + \hat{a}(\hat{\gamma} - \kappa)] \pm \sqrt{c^2[1 - \hat{a}(\hat{\gamma} - \kappa)]^2 + 4\delta(\hat{\gamma} - \kappa)}}{2(\delta - \hat{a}c^2)}. \quad (16)$$

Again we get a condition for these eigenvalues to be real, that is,

$$c \geq \frac{2\sqrt{\delta(\kappa - \hat{\gamma})}}{1 + \hat{a}(\kappa - \hat{\gamma})} \quad (17)$$

which holds if $\kappa > \hat{\gamma}$.

From Eqs. (14) and (16), we will derive constraints on the parameter values in order for the fixed points B and C to be nodes (stable or unstable) or saddle points (i.e., having eigenvalues with different signs), as long as Eqs. (15) and (17) hold. Note that stability corresponds to eigenvalues with positive real part, instead of negative as usual [1], because $t \rightarrow \infty$ implies $z \rightarrow -\infty$. If we look for trajectories with origin at fixed point B we must avoid that it is a stable node (all z -eigenvalues are positive for a stable node), otherwise all of the trajectories in its neighborhood will move towards it. This fact implies that the four eigenvalues in Eq. (14) cannot be positive simultaneously. On one hand, if we deal with predator–prey model (or with competition model with $\gamma < 1$) and inequality $a(1 \pm \gamma) > 1$ holds, then it must be verified that $1 - ac^2 < 0$ and/or $\delta - \hat{a}c^2 > 0$. On the other hand, if we deal with competition model with $\gamma > 1$, then $1 - ac^2 > 0$ and/or $\delta - \hat{a}c^2 > 0$ must be verified.

In addition, fixed point C cannot be an unstable node, but it is easy to see from Eq. (16) that there are not ranges for the parameters for which all of the four eigenvalues (16) are negative.

3.2. Analyzing the leading edge: an approximation

In order to find an analytical expression for the wave front speed, we will focus our attention on the specific but very relevant problem of biological invasions (see Section 4): the species with dimensionless density $n(x, t)$, moves into regions occupied by the species with density $m(x, t)$, where the density of the latter is approximately equal to its saturation value, i.e., $m(x, t) \approx 1$. This approximation will be valid for sufficiently small values of γ

only, since otherwise the interaction among both species would be strong and, as soon as $n \neq 0$, the value of m would change substantially away from its initial value $m = 1$. Then, we can analyze the following equation instead of the coupled system (7)–(8):

$$an_{tt} + \{1 - a[f'(n) \pm \gamma]\}n_t = n_{xx} + f(n) \pm \gamma n. \tag{18}$$

As we shall see in detail below, numerical evidence (Fig. 1) shows that the speed of Eq. (18) is approximately the same as that of the system (7)–(8) for sufficiently small values of γ , as expected. Using the variable $z \equiv x - ct$, with $c > 0$, we see that wavefront solutions with profile $n(x, t) = n(z)$ must satisfy the equation

$$(1 - ac^2)n_{zz} + c\{1 - a[f'(n) \pm \gamma]\}n_z + f(n) \pm \gamma n = 0. \tag{19}$$

First it must be said that, if logistic growth is assumed, the fixed points for Eq. (19) are $(0, 0)$ and $(0, 1 \pm \gamma)$ (in the n_z, n plane), i.e., the approximation $m(x, t) \approx 1$ changes the steady state $(0, 1)$ into $(0, 1 \pm \gamma)$. So, also from this argument, one expects that the lower the value of γ , the better the approximation $m(x, t) \approx 1$. In fact, a low value of γ or Γ is always assumed [1,8–13] because, as mentioned below Eq. (4), such Lotka–Volterra equations rely on the assumption of a weak interaction between both species, which corresponds to keeping only the lowest non-vanishing order in a Taylor series.

Haderer [17] was able to find a remarkable change of variables that reduces the HRDE to a PRDE, and in this way he showed that the speed of the travelling front solutions of Eq. (18) corresponding to heteroclinic orbits connecting the stationary points $(0, 1 \pm \gamma)$ and $(0, 0)$ is given by

$$c = \frac{2\sqrt{f'(0) \pm \gamma}}{1 + a[f'(0) \pm \gamma]}, \tag{20}$$

provided that function f is concave and the following conditions are satisfied:

$$1 - ac^2 > 0, \quad a[f'(0) \pm \gamma] < 1. \tag{21}$$

We stress that in Eq. (20), the positive sign corresponds to the predator–prey model, and the negative one to the competition model.

We must note that the right-hand side in Eq. (20) is the same as that in Eq. (15) when logistic growth is used for source function, i.e., $f(n) = n(1 - n)$. Furthermore, conditions (21) imply that fixed point B is never a stable node, as expected. Eq. (20) can be also derived by means of the variational principle developed by Benguria and Depassier [18] for PRDEs but applied to HRDEs in the same way as it has done in Ref. [12].

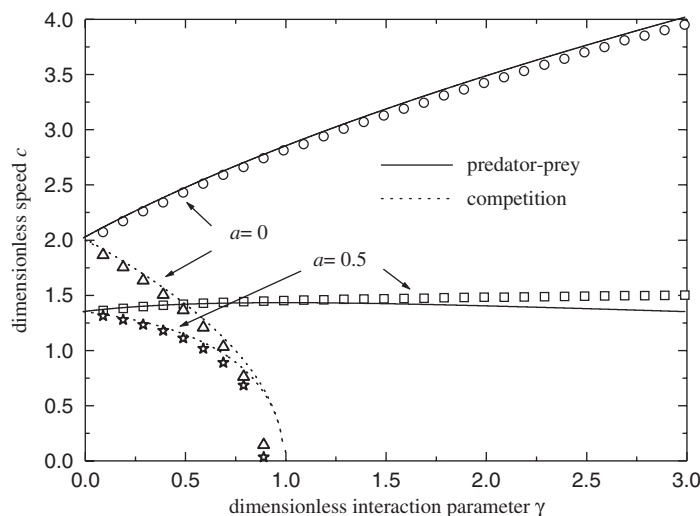


Fig. 1. Comparison between the dimensionless speed predicted by Eq. (20) (curves) and that obtained from numerical integrations of Eqs. (7) and (8) (symbols) for the classical, i.e., non-delayed or PRDE ($a = 0$) and the time-delayed or HRDE ($a \neq 0$) cases. Results are shown as a function of the species interaction parameter γ , both for the prey–predator model and for the competition models (with $\hat{a} = a$, $\hat{\gamma} = \gamma$ and $\delta = \kappa = 1$ for both models). It is seen that the analytical result is more accurate the lower the value of γ , as expected intuitively.

In Fig. 1 we compare the results of Eq. (20) to those obtained from numerical integrations of Eqs. (7) and (8). These simulations are always performed in the same way: with a set of values for the parameters in Eqs. (7) and (8) and with logistic growth for both species, we integrate (7)–(8) numerically over a spatial interval $[0, L]$ large enough (to avoid edge effects) where initially $n = 1 - \theta(x - 0.15L)$ and $m = \theta(x - 0.15L)$, with $\theta(x - 0.15L)$ the usual Heaviside step function with step at $x = 0.15L$. It has been shown [19] that initial conditions with compact support all lead to the same speed for the wavefronts. Non-compact initial conditions, on the other hand, make no ecological sense (see, e.g., Ref. [20]). The values of the parameters used in Fig. 1 are $\hat{a} = a$, $\gamma = \hat{\gamma}$ and $\delta = \kappa = 1$. We can see in Fig. 1 that there is a good agreement between our result (20) and the numerical simulations. Moreover, better agreement is reached the lower the value of γ , as it was to be expected because, as explained above, then the approximation $m \approx 1$ (used to derive (20)) should be more reliable. We also note that the wave front speed is independent of parameters $\hat{\gamma}$ and \hat{a} . We have checked this point also by means of numerical simulations of Eqs. (7) and (8). Note that in the simulations in Ref. [12], only a single equation (similar to (18)) was integrated numerically. In contrast, here we have simulated the whole system (given by Eqs. (7)–(8) in our case). Thus, here a time-delayed reaction–diffusion system with interacting species has been numerically integrated for the first time. This point is rather important, because in contrast to what was done in Ref. [12], it is now possible to determine the accuracy of the analytical prediction for the speed (Eq. (20) for the systems here considered): the accuracy decreases for increasing values of the reduced interaction parameter γ (Fig. 1).

4. Comparison to observations

Here, we will apply the results above to predict front speeds for two biological invasions, and compare to the measured speeds. Both examples below apply to populations living in two-dimensional spaces. Obviously, to get the two-dimensional version of Eqs. (7) and (8), we only have to write the Laplacian ∇^2 instead of the one-dimensional second spatial derivative ($\partial^2/\partial x^2$ or subindex $_{xx}$) in Eqs. (7) and (8). But in polar coordinates, we have that $\nabla^2 \rightarrow \partial^2/\partial r^2$ as $r \rightarrow \infty$ under the assumption that the population densities are independent of the polar angle θ . This will hold provided that the origin of the space coordinates is chosen at the point of origin, or introduction, of the invasive species (with reduced number density n), and that the habitat (diffusive and reproductive parameters) is homogeneous. Thus, all we have to do is to replace the independent variable x by $r \equiv \sqrt{x^2 + y^2}$ in all of our equations above. The validity of this point has been already noted by Murray [1] for other reaction–diffusion systems.

4.1. Predator–prey model

We shall apply the preceding results to the waves of advance of farming populations in the European Neolithic transition. This problem has been tackled previously in Refs. [6,12]. However, these models are less elaborate than the present one. In Ref. [6], the interaction between farmers and hunter-gatherers was neglected altogether. In Ref. [12], it was included as an additional term put by hand in the evolution equation, so the equation for the front speed was different than the result (20), which is an improvement since it has been obtained from carefully derived evolution equations, in contrast to Section 3 in Ref. [12]. Another important difference between the present work and previous one is the following. The value of the interaction parameters γ and $\hat{\gamma}$ in Ref. [12] was taken from Ref. [21], but these were assumed, without any justification, which has led to criticism [22]. In fact, as far as we know, the values of the interaction parameters Γ and $\hat{\Gamma}$ have been never derived previously for any system (even in non-delayed models). This obviously forbids a fair quantitative comparison of the predictions to experimental observations.

We will now introduce a way to derive the values of these parameters. Our idea is very simple: the stronger the predator–prey interaction, the sooner the prey will disappear in a given location. First, note that in our case (Neolithic transition), both parameters Γ and $\hat{\Gamma}$ must have the same value, because the species interaction corresponds to hunter-to-farmer (i.e., ‘prey-to-predator’) conversion. In other words, if the acculturation gives rise to an increase of a given number of farmers, in a given spatial area and during a given time interval (last term in Eq. (1) with the positive sign), this must correspond to a decrease of the same number of hunter-gatherers (last term in Eq. (3)). This was noted already in by Ammerman and Cavalli-Sforza [11]. From Eq. (9)

and $k = 0.032 \text{ yr}^{-1}$, $N_{max} = 100 \text{ farmers km}^{-2}$ and $M_{max} = 1 \text{ hunter km}^{-2}$ [6,11], we find $\gamma = 0.01\hat{\gamma}$. In order to determine the coexistence time by means of numerical integrations performed on Eqs. (7) and (8), we choose a point in the spatial interval where the farmer density initially equals to zero and the hunter density equals to his carrying capacity. In this point we compute the time t_1^* which is defined as that when the farmer density reaches the 1–6% of its carrying capacity, i.e., the moment that farmer population becomes measurable [23]. We also compute the time t_2^* defined as the moment when the hunter density decrease to 1–6% of its carrying capacity, i.e., the moment at hunters become nearly extinct. The numerical coexistence time is just $t_c^* = t_2^* - t_1^*$. The reasons to take the range 1–6% are not arbitrary, in fact in Archaeology not all remains are not recovered (specially the oldest ones) and one can thus detect ancient populations only above a threshold population level which, for Neolithic settlements, has been estimated in the range 1–6% [23]. Our numerical simulations have allowed us to determine the hunter–farmer coexistence time, which we find to be a decreasing function of the dimensionless interaction parameter $\hat{\gamma}$ (see Fig. 2), as was to be expected from the simple argument above. To perform numerical integrations on Eqs. (7) and (8) we also need the values of the other parameters: $k = 0.022 \text{ yr}^{-1}$, $\tau = 12.5 \text{ yr}$, $\hat{\tau} = 13.5 \text{ yr}$, $D = 16.5 \text{ km}^2 \text{ yr}^{-1}$ and $\hat{D} = 24.5 \text{ km}^2 \text{ yr}^{-1}$ [11,6,24]. From the archaeological farmer and hunter-gatherer sites, it is found that the experimental coexistence time t_c varies, but a typical value can be estimated as 100 years (Ref. [11, pp. 59 and 61]). From the definition of t_c^* above Eq. (7), this corresponds to a dimensionless time of $t_c^* = kt_c = 3.2$, where we have used that $k = 0.032 \text{ yr}^{-1}$ [6]; from this and $\tau = 12.5 \text{ yr}$ [6,11], we have that $a = k\tau = 0.4$. These values and the numerical results in Fig. 2 make it possible, for the first time, to estimate a range for the interaction parameters. So we get $\hat{\gamma} = 4.0\text{--}12.4$ and thus $\gamma = 0.01\hat{\gamma} = 0.040\text{--}0.124$. Then we get from Eq. (9) that $\Gamma = (1.280\text{--}3.968) \times 10^{-3} \text{ km}^2(\text{hunter yr})^{-1}$ and $\hat{\Gamma} = (1.280\text{--}3.968) \times 10^{-3} \text{ km}^2(\text{farmer yr})^{-1}$.

Numerical integrations of Eqs. (7) and (8) show that a travelling wavefront exists connecting fixed points B and C . From them, we get that the numerical-integration prediction for the front speed is $v_{num} = 1.036\text{--}1.053 \text{ km yr}^{-1}$, which falls into the range observed from the archaeological record, i.e., $1.0 \pm 0.2 \text{ km yr}^{-1}$ [6].

With this set of parameters it is easy to check that fixed points B and C are both saddle points, which is in agreement with the paragraph below Eq. (17). Since $\hat{\gamma} > \kappa$, only the first of the conditions (15) and (17) must be satisfied, as it indeed occurs. Moreover, conditions (21) hold and this enables us to use Eq. (20) to evaluate the wavefront speed, which yields $v_{app} = 1.047\text{--}1.063 \text{ km yr}^{-1}$. We can observe that the three values for the speed (numerical, experimental and analytical) differ in the worst case only by about 6%.

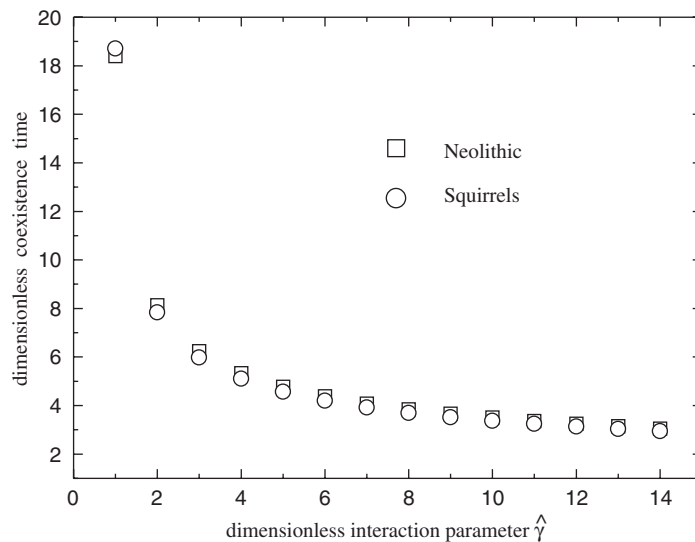


Fig. 2. Dimensionless coexistence time as a function of the species interaction parameter $\hat{\gamma}$, determined from the numerical simulations [23], for the prey–predator model with $\gamma = 0.01\hat{\gamma}$ (Neolithic transition) and for the competition model with $\gamma = 0$ (grey and red squirrels). The values of the other parameters are given in Section 4.

4.2. Competition model

Interspecific competition models have been proposed previously to explain the spatial spread of the grey squirrel (*Sciurus carolinensis*) into British regions occupied by the red squirrel (*Sciurus vulgaris*), and the subsequent extinction of the latter [9]. In the same way as in the previous subsection, we shall make use of the coexistence time to estimate the values of the interaction parameters. In contrast to the former application, in this one we see no justification to assume that both interaction parameters (Γ and $\hat{\Gamma}$) have the same value. But on the other hand, ecologists have noted a negative effect of the interaction on the numbers of the native squirrel but not on those of the introduced one [9,13]. Thus, we shall try to simplify our competition model by setting $\gamma \simeq 0$, so that $\hat{\gamma}$ becomes the single interaction parameter. With this approximation, we find from our numerical simulations that the coexistence time is a decreasing function of $\hat{\gamma}$, as one can see in Fig. 2 and was to be expected. Although it is not necessary to estimate numerically $\hat{\gamma}$ in order to compute the front speed in this very special case, we would like to explain very briefly how the coexistence time can, again, be used to determine the value of $\hat{\gamma}$. The typical coexistence time observed for this invasion is about 16 years [13], which multiplied by the observed growth rate of the greys, namely $k = 0.82 \text{ yr}^{-1}$ [9], yields a dimensionless coexistence time of $t_c^* = kt_c = 13.1$. This leads us to estimate $\hat{\gamma} = 0.89\text{--}1.22$ from Fig. 2. In Ref. [9], the authors determined the values of the other parameters we need: intrinsic net growth rate for the reds $\hat{k} = 0.61 \text{ yr}^{-1}$, and carrying capacities $N_{max} = 1000 \text{ greys km}^{-2}$, $M_{max} = 75 \text{ reds km}^{-2}$. From these and Eq. (9), we can estimate the dimensional parameter $\hat{\Gamma} = 9.98 \times 10^{-4} \text{ km}^2(\text{greys yr})^{-1}$. We now depart from the approach by the authors in Ref. [9], because in order to estimate diffusion coefficients they used experimental value of front speed. Here, we prefer make use of the expression that relates the diffusion coefficient to the mean-square-displacement, namely $D = \overline{\Delta^2}/4T$ (see e.g., Ref. [6]). A realistic estimation for the dispersal range is 1–16 km [25]. Assuming a uniform distribution, the former range leads to $\overline{\Delta^2} = 94 \pm 21 \text{ km}^2$ (we take one standard deviation to estimate the error). We also need the delay time for both species but it is easy to estimate because it is essentially the time needed for a newborn individual to grow into and adult and reproduce himself (during this time the individual does not usually disperse). For both species this time is about 1 year [26]. It has been shown [6] that the delay time in Eqs. (5) and (6) is half of this resting time. Thus, we have $\tau = \hat{\tau} = 0.5 \text{ yr}$ and hence $D = \hat{D} = 94 \pm 21 \text{ km}^2 \text{ yr}^{-1}$. Now that we have estimated *all of the parameter values from independent observations*, we can make a meaningful comparison between theory and experimental observations.

With the set of parameter values above, numerical integrations of Eqs. (7) and (8) yield for the wave front speed $v_{num} = 6.2 \pm 1.4 \text{ km yr}^{-1}$. This range is consistent with the experimental value $v = 7.7 \text{ km yr}^{-1}$ [9,27]. Again both fixed points are saddles and conditions (21) are satisfied, which enable us to use Eq. (20) to determine the wavefront speed. This speed is $v_{app} = 6.2 \pm 1.4 \text{ km yr}^{-1}$, which is again consistent with the value experimentally observed and with the numerical integrations of Eqs. (7)–(8).

5. Discussion

The main new results of this paper are as follows:

- (i) Because the diffusive delay is very important in biological populations [5,7], we have derived the evolution equations for interacting populations with time-delayed diffusion. We have also derived the conditions for extinction and the speed of fronts (Eq. (20)).
- (ii) We have integrated numerically the set of coupled evolution equations (7)–(8), and compared the numerical and analytical front speeds. There is good agreement (Fig. 1).
- (iii) We have introduced a completely new way to estimate the value of the interaction parameter between both species, based on the coexistence time of them after the arrival of the introduced species (Fig. 2).
- (iv) We have compared the predictions of our new formula for the front speed to those observed in real biophysical systems, both for an interaction of the predator–prey type (the Neolithic transition in Europe) and for the competition case (the grey and red squirrels in Britain). In contrast to previous authors [9,21], *our predictions make use of no free or adjustable parameters at all* (because of our new approach summarized in the previous point (iii)). In both cases analyzed, there is reasonably good quantitative agreement between the front speeds predicted by our model and those observed in real systems.

Acknowledgements

We want to thank Prof. A. Ammermann and Prof. N. Soler for helpful discussions about Archaeology and for providing us with Ref. [23]. Computing equipment used has been funded in part by the Generalitat de Catalunya under Grant SGR-2001-00186, and by the MICYT under Grants REN 2000-1621 CLI (J. F.) and BFM 2000-0351 (V. O. C. and V. M.).

References

- [1] J.D. Murray, *Mathematical Biology*, Springer, Berlin, 1993.
- [2] D. Jou, J. Casas-Vázquez, G. Lebon, *Extended Irreversible Thermodynamics*, Springer, Berlin, 1996.
- [3] M. Al-Ghoul, B.C. Eu, *Physica D* 90 (1996) 119–153.
- [4] M. Al-Ghoul, B.C. Eu, *Physica D* 97 (1996) 531–562.
- [5] J. Fort, V. Méndez, *Rep. Progr. Phys.* 65 (2002) 895–954.
- [6] J. Fort, V. Méndez, *Phys. Rev. Lett.* 82 (1999) 867–870.
- [7] J. Fort, V. Méndez, *Phys. Rev. Lett.* 89 (2002) 178101.
- [8] N.S. Goel, *Rev. Mod. Phys.* 43 (1971) 231–276.
- [9] A. Okubo, P.K. Maini, M.H. Williamson, J.D. Murray, *Proc. R. Soc. Lond. B* 238 (1989) 113–125.
- [10] P.C. Fife, *Mathematical Aspects of Reacting and Diffusing Systems*, Springer, Berlin, 1979.
- [11] A. Ammerman, L.L. Cavalli-Sforza, *The Neolithic Transition and the Genetics of Populations in Europe*, Princeton University Press, Princeton, 1984.
- [12] V. Méndez, J. Fort, J. Farjas, *Phys. Rev. E* 60 (1999) 5231–5243.
- [13] J.C. Reynolds, *J. Anim. Ecol.* 54 (1985) 149–162.
- [14] M. Williamson, *The Analysis of Biological Populations*, Edward Arnold, London, 1972.
- [15] V. Ortega-Cejas, J. Fort, V. Mendez, *Ecology* 85 (2004) 258–264.
- [16] Note that these equations are very similar to those considered in Ref. [12, Section 5]. The differences are the appearance of new terms with the temporal derivatives of the additional species in the right-hand side, and of terms due to the interaction in the left-hand side. All of these changes come from taking into account the interaction terms from ‘first principles’, i.e. in the balance equations for number densities, Eqs. (1) and (3), which was not done in Ref. [12]. Instead, there a single interaction term was added by hand to the final evolution equation in a phenomenological, and therefore less rigorous, way.
- [17] K.P. Hader, *Can. Appl. Math. Q.* 2 (1994) 27–43.
- [18] R.D. Benguria, M.C. Depassier, *Phys. Rev. E* 57 (1998) 6493–6496.
- [19] D.G. Aronson, H.F. Weinberger, *Adv. Math.* 30 (1978) 33–76.
- [20] M.G. Neubert, H. Caswell, *Ecology* 81 (2000) 1613–1628.
- [21] S. Rendine, A. Piazza, L.L. Cavalli-Sforza, *Am. Nat.* 128 (1986) 681–706.
- [22] A.G. Fix, *J.R. Anthropol. Inst.* 2 (1996) 625–643.
- [23] Three different and completely independent examples (number of sites in the Lower Diyala region, in the Warke region and settlement area at the site of Knossos) yield values in the range 1–6% (the precise values are 5.5%, 5% and 1.5%, respectively). See A. Ammermann, L.L. Cavalli-Sforza, D.K. Wagener, in: E.B.W. Zubrow (Ed.), *Demographic Anthropology. Quantitative Approaches*, School of American Research, Santa Fe, 1976, pp. 36 and 48. A less precise value of about 1% has been also estimated from an additional example (number of houses in the Aldehoven Platte) by Ammermann and Cavalli-Sforza in [11], pp. 73–74.
- [24] J. Fort, T. Pujol, L.L. Cavalli-Sforza, *Cambridge Archaeol. J.* 14 (2004) 53–61.
- [25] <http://spot.colorado.edu/~halloran/sq_grey.html>.
- [26] <<http://www.squirrels.org/gray.html>>.
- [27] M. Williamson, K.C. Brown, *Phil. Trans. R. Soc. Lond. B* 314 (1986) 505–522.